An Objective Study of 500-hPa Moving Troughs in the Southern Hemisphere

EVERSON D. PIVA

Centro Regional Sul de Pesquisas Espaciais, Instituto Nacional de Pesquisas Espaciais, Santa Maria, Brazil

MANOEL A. GAN AND V. BRAHMANANDA RAO

Centro de Previsão de Tempo e Estudos Climáticos, Instituto Nacional de Pesquisas Espaciais, São José dos Campos, Brazil

(Manuscript received 4 January 2007, in final form 24 September 2007)

ABSTRACT

The location and movement of 500-hPa troughs using an automated method are studied with data from a 24-yr period with the objective of determining the trough formation and dissipation regions in the Southern Hemisphere. To identify the 500-hPa mobile troughs, an objective method that uses the Eulerian centripetal acceleration (ECA) is developed. On average, 868 troughs per year were identified by the method, with an increase in trend during the period studied. The troughs have an average lifetime of 4.3 days, being longer (shorter) in subtropical (high) latitudes. The average calculated phase velocity was 13.6 $m\,s^{-1}$, being higher (lower) in middle (high) latitudes. The troughs are normally found in the 60°–40°S latitudinal band, with maximum occurrence at 50°S. The longitudinal distribution of trough genesis has three maximum regions: over the Drake Strait and the South Atlantic Ocean, over the Indian Ocean around 50°S, and over the southwestern Pacific Ocean between 150°E and 150°W. The trough dissipation regions are less concentrated than the genesis regions and also show three maxima: over the west of the Andes, south of the African continent, and south of Australia. The seasonal variation in the trough dissipation shows that the 30°–40°S band is more active during winter than in summer. The difference between the genesis and dissipation location is that formation occurs more in middle and high latitudes, while dissipation is more common in the 40°–30°S latitude belt.

1. Introduction

Even a cursory analysis of the geopotential height in the mid- and upper troposphere shows the presence of waves with wavelengths varying from planetary scale to mesoscale. These waves have a fundamental role in maintaining the heat, momentum, and moisture balance and might generate cyclones at the surface level. In general, the initial formation of surface cyclones or cyclogenesis in the Southern Hemisphere (SH) occurs between 35° and 55°S. The matured systems are found between 50° and 60°S, and the dissipation occurs to south of 60°S. The cyclones that form in the mid- and high latitudes move east while those that form close in the subtropical latitudes move southeast, forming a close spiral (Streten and Troup 1973; Physick 1981; Sinclair 1995; Rao et al. 2002).

A few studies have been made regarding the 500-hPa cyclones in the SH. Keable et al. (2002, hereinafter KEA02) made a climatological study of cyclones at 500 hPa using 40 yr (1958 through 1997) of data. They used the methodology developed by Murray and Simmonds (1991) and improved by Simmonds and Murray (1999). Their results show that throughout the year there is a high density of cyclones in the latitude of the circumpolar trough with secondary maxima in the Chaco region and west coast of South America. Cyclogenesis regions are observed over Antarctica and New Zealand, and over the tip of South America. Cyclolysis is observed over Antarctica with secondary maxima over the Pacific Ocean around 40°S. The oceanic regions to the north of 60°S are characterized by higher formation than dissipation, while the opposite is noted in the 10° belt near Antarctica. Regarding the interannual variation they noted that in the 1970s and up to the mid-

Corresponding author address: Manoel A. Gan, Instituto Nacional de Pesquisas Espaciais, Centro de Previsão de Tempo e Estudos Climáticos, Caixa Postal 515, 12201-970, São José dos Campos, SP Brazil.
E-mail: alonso@cptec.inpe.br

DOI: 10.1175/2007MWR2135.1

1980s there was a reduction in the number of cyclones, and in the 1990s an increase occurred, but the number of cyclones is less than that observed in the 1960s.

In a recent article Fuenzalida et al. (2005) made a climatological study of cutoff lows at 500 hPa in the SH using 31 yr (1969–99) of data of National Centers for Environmental Prediction–National Center for Atmospheric Research (NCEP–NCAR) reanalysis. Their results show a total of 1253 lows with a mean of 40 cases per year. Closed lows seem to occur near the continents in the latitude band of 20°–50°S with a maximum at 38°S. They noted a strong annual variation near South America and Africa, with minimum in the summer and maximum in the winter, while over Australia the opposite occurred.

In the case of South America, Gan and Rao (1996), Innocentini and Caetano Neto (1996), Piva (2001), and Vera et al. (2002) noted the presence of troughs in the middle and upper troposphere associated with surface cyclogenesis. Seluchi (1995) showed that the perturbation responsible for the cyclogenesis can be identified 5 days earlier by a long wave and a higher baroclinic zone around 35°S. The intensification of the baroclinic zone occurs because of hot and humid air blowing to southern South America crossing Paraguay and North Argentina.

One of the early studies regarding the troughs in the midtroposphere for the Northern Hemisphere (NH) was by Sanders (1988) using 9 yr of National Meteorological Center (NMC) data. He identified 8–15 troughs per week in the formation stage and 3–18 during the dissipation. He also found a median life period of 12 days, with a mode of 5 days. Sanders (1988) found that the troughs form over the continents where the meridional wind is northerly and dissipate where the meridional wind is southerly. He found two principal regions of formation over the mountains or downstream while the three principal regions of dissipation were on the upstream side of the mountains.

Another climatological study of moving troughs in the midtroposphere in the NH was made by Lefevre and Nielsen-Gammon (1995, hereinafter LN95). They used the NMC 12-h gridded analysis for the period of 1969 through 1988. Their results show that the average lifetime of troughs was 5.3 days with a median of 4 days, which depends on the latitude.

The purpose of the present paper is to study the location and movement of troughs at 500 hPa using an automatic method and applying it to a 24-yr (1 March 1979–28 February 2003) collection of data with the objective of determining the formation and dissipation regions. The climatology of troughs, which are the first indication of surface cyclogenesis (Sanders 1986, 1988), should be useful for the forecaster. In this context the present study is different from earlier studies (Gan and Rao 1996; Vera et al. 2002; Fuenzalida et al. 2005), particularly in the Southern Hemisphere, because they are focused on closed cyclones, which are a stage after the initiation of surface cyclogenesis. The present study is also different from previous Southern Hemisphere studies because we developed an objective method that uses the Eulerian centripetal acceleration (ECA) variable to identify the 500-hPa troughs. This variable, defined by LN95, was already used for the NH, allows a better identification of the troughs in midlatitudes, and is different from the work of KEA02, which included open and closed cyclonic circulation.

2. Data and methodology

In the present study we used the 6-hourly gridded data from the NCEP–NCAR reanalysis for the period from 1 March 1979 to 28 February 2003. We used data from 1979 because after this year the satellite observations improved the quality of data. The variables used were the geopotential height (gpm), and zonal and meridional wind components ($m\,s^{-1}$) at 500 hPa. A detailed description of the NCEP–NCAR dataset is given by Kalnay et al. (1996). Some comments are in order regarding several problems that occurred when the NCEP–NCAR reanalysis was performed. Some improvements were made regarding the surface pressure [Paid Observation (PAOBS) problems between 1979 and 1992], snow cover analysis, humidity diffusion, oceanic albedo, cloud tuning parameters, and snowmelt in the NCEP–Department of Energy (DOE) reanalysis version (Kanamitsu et al. 1999). Simmonds (2003), using both the NCEP–NCAR and NCEP–DOE reanalysis, had shown some differences in surface cyclone activity over the Southern Ocean depending on the reanalysis dataset used. The Hodges et al. (2003) study compared the storm-track statistics based on four reanalysis projects [European Centre for Medium-Range Weather Forecasts (ECMWF), NCEP–NCAR, NCEP–DOE, and National Oceanic and Atmospheric Administration (NOAA)] and found significant differences in the level of cyclonic activity (upper and lower levels) between the reanalysis datasets, concluding that there is much greater uncertainty in location and intensity systems in the SH than in the NH. For example, in SH wintertime, the 250-hPa cyclonic activity in the Australian subtropical jet region is better defined in NCEP–NCAR than the 15-yr ECMWF reanalysis (ERA-15). Thus, some differences between our results and other studies using another reanalysis dataset can be anticipated.

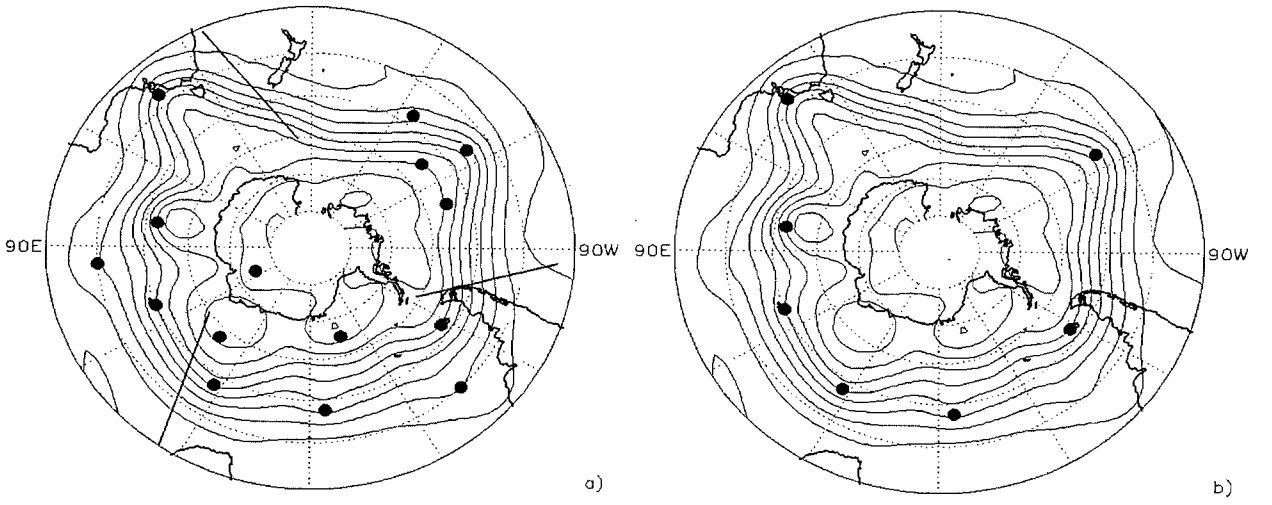

FIG. 1. The 500-hPa geopotential height (contours every 100 gpm) at 1200 UTC 17 Feb 1999. (a) The filled circles identify minima of ECA values. (b) The filled circles identify troughs found when all the criteria are considered. The straight lines in (a) represent the position of the stationary wave ridge axis identified by Van Loon and Jenne (1972).

The 500-hPa level was chosen to study the trough climatology because of the relationship between trough and surface cyclogenesis, and because the level of 500 hPa has been shown to be ideal for identifying the upper-tropospheric mobile troughs that affect the lower troposphere (LN95). In addition, it also facilitates the comparison of this trough climatology with previous studies.

To identify the 500-hPa mobile troughs we developed an objective method that uses the ECA [Eq. (1)]. According to LN95, this variable better identifies the mobile troughs because it can be interpreted as the transport of the curvature vorticity by the geostrophic wind, which is located upstream of the cyclonic vorticity advection regions. Physically, ECA represents the centripetal acceleration experienced by an air parcel following the geostrophic streamlines. Because the ECA is the result of the curvature term of the vorticity, it can identify the cyclonic circulations better than the relative vorticity. The advantage of the ECA calculation is due to the fact that the regions of ECA maxima in NH or minima in SH correspond to the features that a synoptician could identify as mobile troughs (LN95):

$$\mathrm{ECA} \equiv V_g^2/R_s. \tag{1}$$

Here, V_g is the geostrophic wind magnitude and R_s is the curvature radius of the geostrophic flow.

An example of the ECA minima (black dots) associated with the 500-hPa geopotential height field is shown in Fig. 1a. The wavenumber-5 pattern in midlatitudes is verified with some shorter waves, as obtained by Salby (1982). From this figure it can be seen that the method is very sensitive to the change of flow curvature as indicated by the trough identification over the South Atlantic Ocean at 45°S, 10°W and over the southeastern Pacific at approximately 55°S, 110°W. The criteria used in the objective method are the minimum lifetime, the intensity of the ECA minimum, and the latitudinal thresholds of the trough position. In the case of lifetime, the troughs must be identified for at least 2 days continuously. In the intensity requisite, the ECA value at the trough must become either equal or inferior to -4.0×10^{-4} m s^{-2} in at least one analysis, as suggested by LN95. With the minimum southern latitude criterion we disregarded the troughs that remain more than 24 h in latitudes north of 30°S. In Fig. 1b we can see the troughs identified by the method when we consider all of the criteria presented above.

The results shown in the figures are in regards to the trough appearance frequency, genesis, and dissipation, and difference between genesis and dissipation, and all of them are normalized with respect to an area equal to 5.5×10^4 km^2 (which corresponds to an area of 2.5° latitude and longitude located at 45°S) and smoothed with a nine-point filter. The trough appearance represents the collection of all points occupied by the trough during its lifetime, including the genesis and dissipation.

The tracks of the troughs found at time t are obtained with an algorithm that is based on finding the trough position at time $t + 6$ h. To determine this estimated position of the trough at time $t + 6$ h we used the average of the flow velocity in the region occupied by the trough on time t and the mean velocity of the

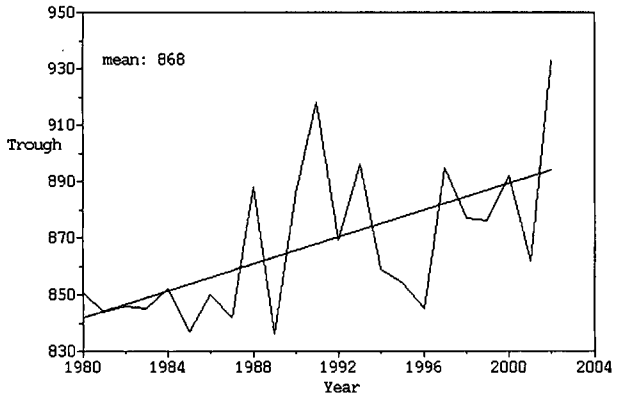

FIG. 2. Troughs for the year. The straight line shows the trend for the period.

troughs reported in literature, which is found to be approximately 14 m s^{-1} (Sanders 1988; KEA02). Such a procedure was adopted because in many cases the background wind flow is stronger than the displacement speed of the troughs (Palmén and Newton 1969), locating the estimated position far away from the real position.

Normally, detecting the correspondence between the positions of the same trough in two successive time charts is easy and direct. However, there are situations where this correspondence became difficult. We identified the six possible situations; there are three situations for one trough at time t: 1) there is just one trough at time t + 6 h, 2) there are no troughs at time t + 6 h, indicating that the trough dissipated at time t, or 3) there are two troughs at time t + 6 h, in which case we choose just one and the other is discarded; there are two situations for two troughs at time t: 4) either there is one trough at time t + 6 h, in which case we choose one trough and discard another at time t, or 5) there are two troughs at time t + 6 h, in which case we choose the two troughs; and there is one trough at time t + 6 h, which does not find correspondence at a previous time t, indicating that it formed at t + 6 h. In situations 3, 4, and 5 it was necessary to make choices from several possible associations, which depend only on the difference between the estimated and true positions.

Some studies (Karoly 1989; Rao et al. 2002; and others) have shown that the SH circulation is strongly influenced by El Niño (EN) and La Niña (LN) phenomena. To verify whether there is any influence of EN and LN phenomena on the trough behavior, we made composites for EN and LN years. The criterion used to make this composite was that the South Oscillation index during the 3 months of each season should have values higher than 0.5 or less than −0.5 to be considered as EN or LN events, respectively. We selected seven spring [September–November (SON)] and seven summer [December–February (DJF)] seasons with EN and LN. The EN years selected were 1982/83, 1986/87, 1987/88, 1991/92, 1994/95, 1997/98, 2002/03; and the LN years were 1983/84, 1984/85, 1988/89, 1995/96, 1998/99, 1999/00, and 2000/01. The years without EN or LN phenomena were classified as neutral years (NY). The fall and winter seasons were discarded because just a few years had South Oscillation indexes superior to 0.5 or inferior to −0.5.

3. Results

The total mobile troughs identified in SH during the period of 24 yr were 20 821 (Fig. 2). Separating by season, winter [June–August (JJA)] has a higher frequency of troughs with 240 troughs on average (Fig. 3b) and summer (DJF) has only 186 troughs (Fig. 3a). Such a result was expected because the cyclones at surface have a behavior similar to the troughs (Sinclair 1997; Simmonds and Keay 2000a,b).

The average trough frequency per year is 868, which is less than the value noted in other studies. For NH, LN95, using the same variable (ECA) as in our study, found an average of 1373 troughs per year, that is, 37% more than those in SH. KEA02 do not clearly comment about the average trough frequency per year in SH, but because they observed about 19 cyclones in the SH daily analysis, and considering that these cyclones have

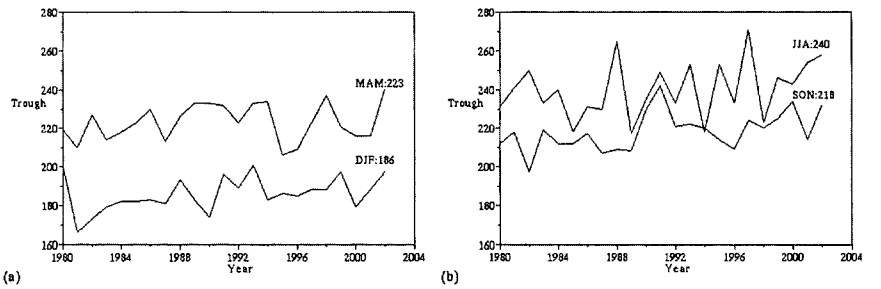

FIG. 3. Troughs for the year for (a) DJF and MAM and (b) JJA and SON.

a mean life of 4 days, we can estimate the frequency as 1729 troughs per year. One of the reasons for the trough number discrepancy between these two studies is that KEA02 consider cyclones as being both closed (vortex) and open (trough) cyclonic circulation. Thus, it is possible that in their methodology one can count a system more than once, that is, a vortex in higher latitudes and a trough in lower latitudes. Another possibility is that we considered just troughs with lifetimes equal to or more than 48 h, while KEA02 limited the lifetime to 24 h. This time threshold difference of 24 h and the different algorithms could have left out many troughs from the present statistics. It should be mentioned that the details of the troughs found in our climatology depend on the specific threshold chosen for the ECA (that indicate the flow curvature) in addition to the other parameters and techniques used in the objective method. For example, when we consider the minimum lifetime of a trough as being 24 instead 48 h, the trough number in 1999 increases from 876 to 1384. This value is lower than the estimated value of the trough number per year by KEA02's study. When we consider the minimum lifetime of 48 h again, and that the trough, during its lifetime, should reach an ECA value equal or less than -3.3×10^{-4} m s^{-2} instead of -4×10^{-4} m s^{-2}, the trough number in 1999 increases to 884. If we reduce the minimum ECA value to -3.0×10^{-4} m s^{-2}, it would increase the trough number to 901. This shows that the threshold of the intensity does not modify the number of the troughs identified much, but the duration of the lifetime has a stronger impact. Even with these changes in the thresholds, the trough number in our case is still less than the number obtained by KEA02. This difference is mainly because, as we mentioned earlier, KEA02 have included both open and closed cyclonic circulation to identify the cyclones in their study, while in our case we considered only troughs, excluding closed cyclones.

The trend analysis of the 20 821 troughs shows an increase of the mobile trough number in the 24 yr (Fig. 2) in SH, especially after 1986. Using the Mann–Kendall test (Gilbert 1983), this tendency becomes 95% significant after 2000. A positive tendency is also verified when we separate the trough series by season (Fig. 3), and the tendency is significant at the 95% level for only summer and spring. Pezza et al. (2007) found similar behavior for the trends of surface cyclones and anticyclones in SH, but the slopes are greater during the summer than winter. Key and Chan (1999) observed different seasonal trends for cyclone number formed in the SH midlatitudes. Their results show that the highest trend of cyclone number occurs in SON, and DJF has a negative trend. On the other hand, Wang et al. (2006) showed that the cyclonic activity trend varies depending on the region. They observed a positive trend of strong cyclone activity in boreal winter over high latitudes of the North Atlantic and over the midlatitudes of the North Pacific, in addition to a negative trend over the midlatitudes of the North Atlantic.

Analyzing the trough frequency, we did not find any relationship with the occurrence of EN or LN phenomena. As well, in our study we did not find a relation between the trough number in the 1980s and 1990s with the Pacific decadal oscillation (PDO), although Pezza et al. (2007) have found a link between cyclone and anticyclone trends with PDO phase.

Studies of surface cyclones have shown a reduction in number in recent years, while the intense cyclone frequency has been on the increase (Simmonds and Keay 2000a,b; Pezza and Ambrizzi 2003). Because one characteristic of intense cyclogenesis at the surface is the reduction of upper-level trough wavelength (Uccellini 1990), the increase of intense cyclones probably can be associated with the increase in number of upper-level troughs, as illustrated in Fig. 2, where the trough frequency per year increases from 850 in the 1980s to 890 in the second half of the period of our study. A similar result was found by Key and Chan (1999) and Lim and Simmonds (2007) when they analyzed the cyclone frequency at both the surface and 500-hPa levels for the entire globe during the period from 1958 to 1997 using NCEP–NCAR reanalysis data, and the number of 500-hPa cyclones in ECMWF reanalysis data for the period from 1979 to 2001, respectively. It is also important to remark that both the quantity and quality of data over the Southern Hemisphere have increased during these 24 yr, improving the reanalysis quality and allowing the identification of more surface cyclones (Simmonds and Keay 2000b). A similar explanation may be given to the analysis of the 500-hPa trough trend.

Considering the trough lifetime, the majority of the troughs have lifetimes of less than 5 days (Fig. 4), with an average and a median of 4.3 and 3.5 days, respectively. However, some troughs have lifetimes of longer than 2 weeks. In the NH, LN95 observed an average lifetime of 5.3 days and a median of 4 days.

An important characteristic of trough lifetime is that it is dependent on the latitude band and season (Table 1). To clarify this point we separate a trough lifetime in the following three latitudes bands: high latitudes (HL; 80°–62.5°S), midlatitudes (ML; 60°–42.5°S), and subtropical latitudes (SL; 40°–20°S). The HL band has the shortest trough lifetime, while the SL the longest. Similar results were found by LN95 for NH.

Regarding the seasonal variation, the shorter trough lifetime occurs in the winter, increasing during the tran-

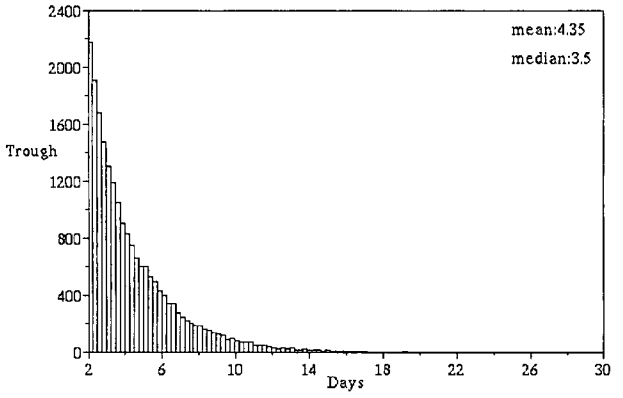

FIG. 4. Trough lifetimes (days).

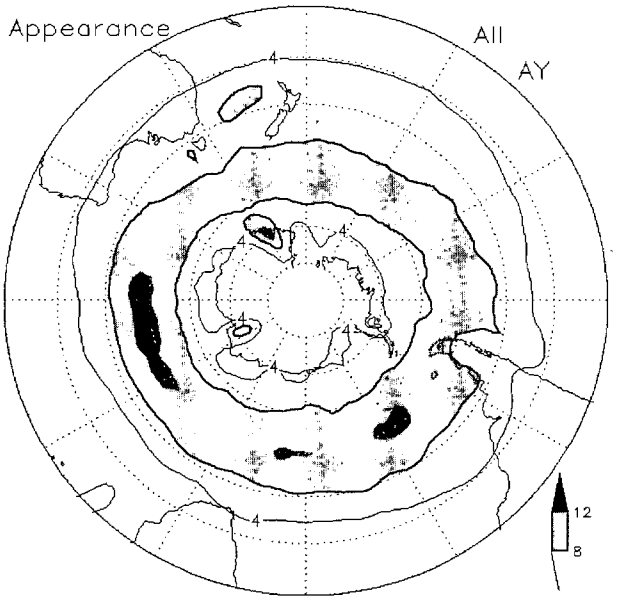

FIG. 5. Appearance of troughs for a year. Areas where the isolines are more than eight troughs per year are darkened.

sition seasons, and reaching the maximum in the summer. However, the difference between the shorter and the longer lifetimes at the same latitude band is not much higher. LN95 showed that troughs have longer lifetimes in the autumn and shorter lifetimes in the summer and winter; however, the difference between the longer and shorter lifetimes is just 0.2 days, which is considered insignificant. An interesting feature of the seasonal variation of the basic state in the SH is the presence of two jet streams during JJA and SON (Carmo 2004). Under such conditions we expect that the waves can have behavior that is different compared to that with one jet stream. On the other hand, it is known that the interseasonal difference in the SH is smaller than in the NH due to the balancing effect of the ocean.

In the winter season and higher latitudes the baroclinicity is high, and eddy potential energy can be converted to eddy kinetic energy more rapidly, inducing a rapid evolution of the system and a shorter lifetime (Gutowski et al. 1992). On the other hand, as the colder (hotter) latitudes and seasons present troughs with shorter (longer) lifetimes in the SH, we can suppose that other effects, such as barotropic conversion, are important; in any case, further studies are necessary to elucidate these differences.

The spatial distribution of mobile troughs (Fig. 5) shows that they are normally present between the Antarctic continent edge (70°S) and 30°S, with four maxima located as follows: one over Antarctica at 160°E and other three along 50°S, extending over the Indian Ocean (50°–100°E), the Atlantic Ocean (30°–40°W), and the 0°–5°E sector. The maxima of mobile trough appearances along 50°S are strongly related to the maxima of the annual average zonal wind (Trenberth 1991), and with the stationary cyclone observed by Inatsu and Hoskins (2004). On the other hand, close to New Zealand, between 30° and 40°S, a minimum of trough appearances is observed with less than eight mobile troughs per year. This region is one that normally has no suitable conditions for developing a transient system, mainly in wintertime, because we can see in the Eady growth rate at the 780-hPa level (Fig. 6) that it has a minimum over this region. This result agrees with Inatsu and Hoskins (2006) who found a storm-track activity minimum in wintertime associated with the split

TABLE 1. Trough lifetime for latitude band and for season.

	Trough lifetime (days)		
Season	HL	ML	SL
DJF	3.6	4.8	5.0
MAM	3.5	4.6	4.9
JJA	3.3	4.0	4.3
SON	3.6	4.3	4.6

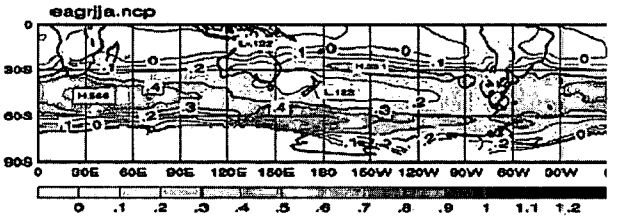

FIG. 6. Eady growth rate at the 780-hPa level, averaged over the period of 1961–2000 from the NCEP–NCAR reanalysis dataset for the SH winter (JJA) [adopted from McBride et al. (2005)].

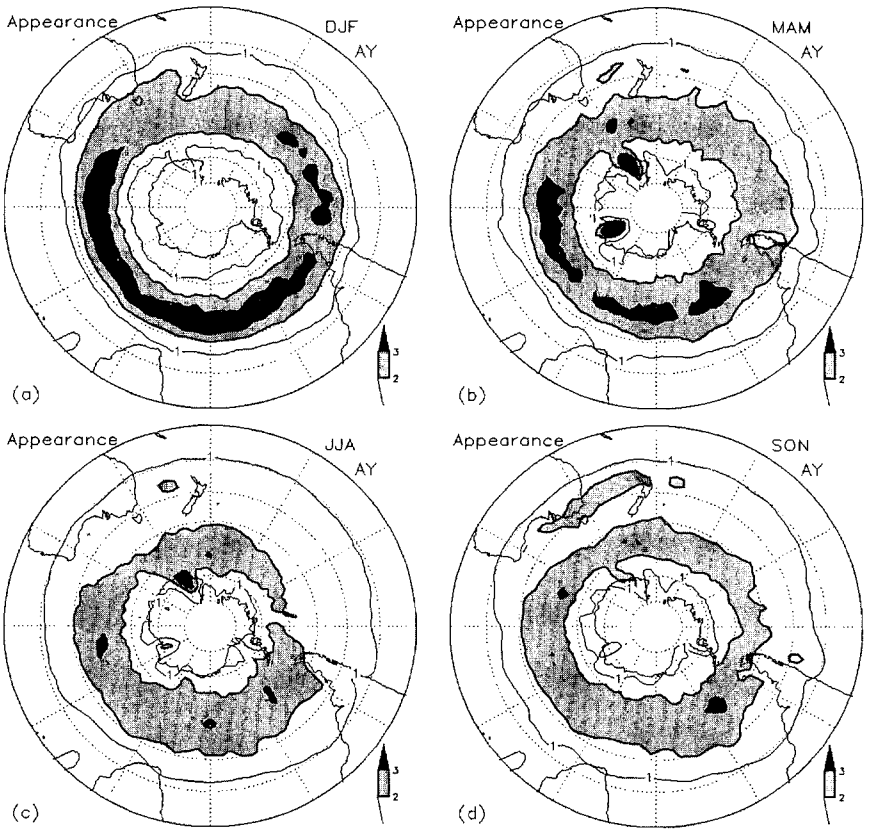

FIG. 7. Trough appearance for season for (a) DJF, (b) MAM, (c) JJA, and (d) SON. Isoline for one trough by season and shaded for two and three troughs by season.

jet over this region, located near the New Zealand region. This region is also associated with a minimum of zonal wind and a maximum frequency of blocks (Marques 1996). A similar feature also occurs in the other seasons and is discussed in the subsequent paragraphs. Another interesting observed feature is the southward displacement of a large number of troughs to the polar region when they are crossing the Andes, probably due to the mountain effect, as noted by Rao et al. (2002).

The trough appearance for each season is illustrated in Fig. 7. We can see in this figure that the latitudinal extension of the region with more than one trough by season decreases during the summertime months (DJF), but it remains in the 60°–35°S belt. Despite the reduced latitudinal extension of the trough appearance during the summer, the region with more than three troughs by season is higher than in other seasons, extending from the southeastern Pacific Ocean to the south Indian Ocean, crossing the Atlantic Ocean at 50°S. Over the Indian Ocean and South Atlantic regions there are maxima in all seasons along 50°S, with the former being the most intense region. The latitudinal concentration of trough appearance during DJF causes the false impression that this season has more troughs, but it is important to point out that DJF is the season with a smaller trough quantity (Fig. 3). The minimum trough appearance in DJF and the two branches over New Zealand in the other seasons are consistent with the minimum wind average field in this region. The trough appearance during March–May (MAM) has a higher frequency and the maximum extends over a large region, with the maximum center larger than in JJA. This result agrees with the results of Rao et al. (2002), who noted that the storm tracks are more intense in the autumn season. During the period of DJF–MAM, the trough appearance tends to be restricted in the subpolar jet stream region, at approximately 50°S, while in the period of JJA–SON the subtropical jet stream at approximately 30°S tends to displace the troughs toward equator, spreading the trough region between these two jet streams (Nakamura and Shimpo 2004). Another interesting characteristic is that the trough appearance increases over Antarctica during the autumn and winter months in the 160°–60°E longitude range.

Comparing Fig. 7 with the 250-hPa statistics obtained by Hoskins and Hodges (2005, their Fig. 10) we can notice that both figures have a good resemblance, but some differences are also found. Our results show a minimum over New Zealand in the DJF season, while the results of Hoskins and Hodges (2005) show a secondary maximum. In JJA, SON, and MAM, their results show a secondary maximum in subtropical latitudes; in our results only a weak signal appeared in the Australian–New Zealand sector. The major difference probably occurs over the east Pacific and to west of the Antarctic Peninsula, where our results show the area of weak trough activity, while in the Hoskins and Hodges (2005) results there is a very active area. Similar to what we noted, they found that in MAM (SON) the statistics are similar to DJF (JJA).

The maximum of the 500-hPa mobile troughs along 50°S is displaced 10° to the north of the maximum of cyclones at the surface located along 60°S, as observed by Sinclair (1997), Simmonds and Keay (2000a,b), and Lim and Simmonds (2007) for the SH and LN95 for the NH. This result is expected because the surface cyclones form in the region between the trough and the ridge, with the troughs located equatorward of the surface cyclones, resulting in a northwestward (in SH) vertical tilt similar to that identified by Grotjahn (1996). Lim and Simmonds (2007) studied the vertical organization of the SH winter extratropical cyclones with the 40-yr ECMWF reanalysis. They discovered that about 80% of the cyclones presented westward vertical tilts. In the 30°–60°S latitude band from the eastern Indian Ocean to the western Pacific Ocean, a number of cyclones tend to have a strong component of northward vertical tilt, whereas the cyclones over the Atlantic and Pacific in the 30°–45°S latitude band have southward tilts.

The analysis of trough genesis (Fig. 8) shows that the midlatitudes and some specific regions of the Antarctica continent are preferential regions. The values higher than 0.65 troughs per year are found over the Drake Strait–South Atlantic Ocean, the Indian Ocean near 50°S, and the southwestern Pacific Ocean between 150°E and 150°W. Over Antarctica, the maxima are found at 150° and 70°E. According to Sanders (1988) and LN95, the trough genesis is more frequent on the east side of the stationary long-wave ridge. This can also be seen in Fig. 8 taking into account the position of the wavenumber-3 ridges found (Fig. 1a) by Van Loon and Jenne (1972) and Yasunari (1977) in the SH, located close to 45°E, 170°E, and 70°W. LN95 found that the trough genesis regions in NH are located downstream of large mountain barriers. Because in SH the

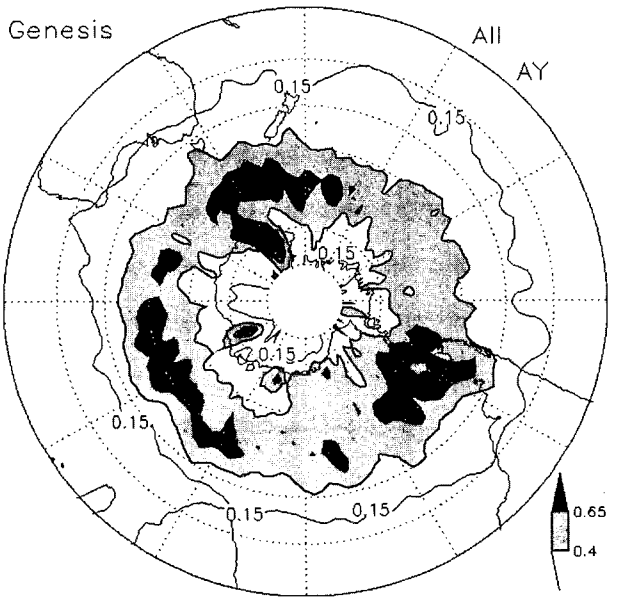

FIG. 8. Trough genesis per year. Isolines are for 0.15, 0.4, and 0.65 troughs per year. Areas where the isolines are more than 0.4 troughs per year are darkened.

mountain chains are not much higher in the midlatitudes, with the exception of the Andes, we expect that the trough formation cannot be influenced by the orography. Although a strong trough–orography relationship probably occurs over the Antarctica continent, close to 150° and 70°E, there is an accentuated topographical change at both longitudes (Van Loon 1965). On the other hand, some studies have shown that the Antarctic continent has a strong influence over the SH flow (James 1988, 1989; Watterson and James 1992; Juckes et al. 1994). James (1988), using the barotropic vorticity equation on the sphere, has shown that during winter the location and strength of the jet split over south Australia and New Zealand are largely due to the morphology of the Antarctic continent, because the Antarctic orography can excite waves (with long wavelength) that propagate equatorward and reach the midlatitudes of the SH. According to James (1989), the persistent Antarctic drainage flow can reduce the cyclonic vorticity over the polar cap in upper levels and exports cyclonic vorticity to lower latitudes. With a linear baroclinic model, Watterson and James (1992) also found that the Antarctic orography generated a large-scale Rossby wave that propagated to the southern subtropics, but the response was weaker than for the James (1988) model.

The latitudinal distribution of the trough genesis (figure not shown) indicates a primary maximum around 52.5°S and a secondary maximum at 70°S. The reduction of trough genesis is higher toward the equator than

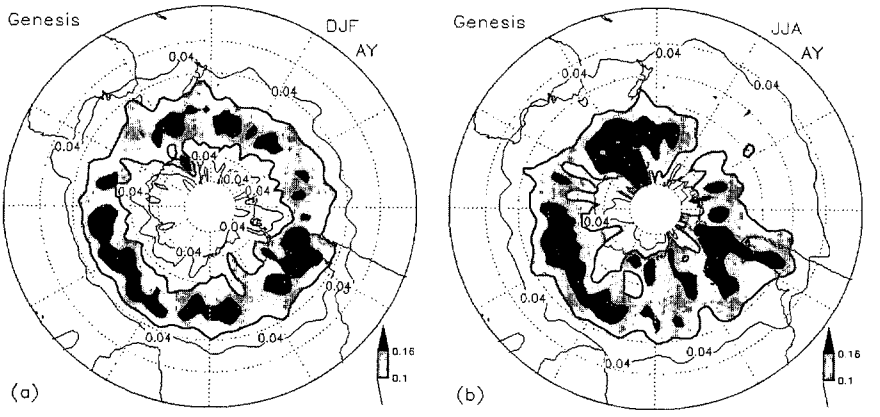

FIG. 9. Trough genesis for season for (a) DJF and (b) JJA. Isolines are for 0.04, 0.1, and 0.16 troughs by season. Areas where the isolines are more than 0.1 troughs by season are darkened.

the polar region. The longitudinal distribution (figure not shown) presents three preferential regions located close to 60°E, 150°E, and 60°W, showing a possible relationship with wavenumber 3.

The seasonal variability of the trough genesis (Fig. 9) shows that the Antarctic region is less active and the South Pacific between 150° and 80°W is more active in summertime. Comparing the pattern of trough genesis for each season with the annual pattern (Fig. 8), we can see that the highest differences are found in DJF. It is possible to observe an almost-continuous zonal band of trough genesis higher than 0.16 troughs by season. This result corroborates with Chang (2000) who observed that the downstream development (DSD) is more important in summer, once the baroclinic instability is lower and becomes concentrated in a reduced latitude band in this season.

Comparing our trough genesis results for summer and winter with KEA02's results, we can observe some agreements and differences. The differences are that in KEA02 there is a maximum of trough genesis over Antarctica in both seasons, while in our study it is observed only in winter (Fig. 9). During the summer, a maximum of genesis was found around 65°S, extending from 0° to 90°E in KEA02's results, while in our study this region is more toward the equator, around 50°S. Such differences can be explained, in part, by differences in the methodology. Because it is common to observe a trough in lower latitudes associated with a cyclone in higher latitudes in the geopotential height field, there is a tendency that the maximum trough frequency in KEA02 could be located more toward the polar region. An agreement of both studies occurs over the Pacific Ocean around 40°S, where we observe more trough genesis during the wintertime. Perhaps the result that agrees better occurs over the Drake Strait during the winter, where the maximum of trough genesis extends to equator along South America. The wintertime results show good agreement with the study of Hoskins and Hodges (2005), in which the genesis density field also presented three areas of maximum.

The dissipated trough phase (the end of the trough life) has an extended region (Fig. 10) and it is less concentrated in some regions than in trough genesis. This region extends from the edge of Antarctica to 30°S, with three maxima observed upstream of the Andes, over southern Africa, and south of Australia. Because the dissipation of the trough region does not present many concentrated areas, we can infer that the duration

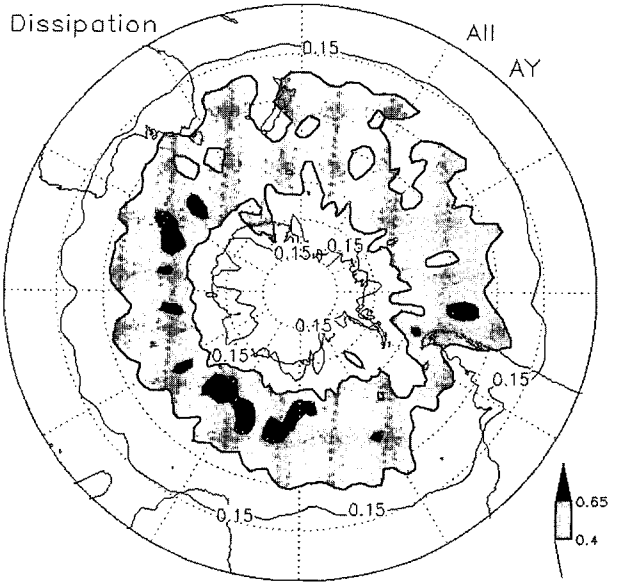

FIG. 10. Trough dissipation for a year. Isolines are for 0.15, 0.4, and 0.65 troughs per year. Areas where the isolines are more than 0.4 troughs per year are darkened.

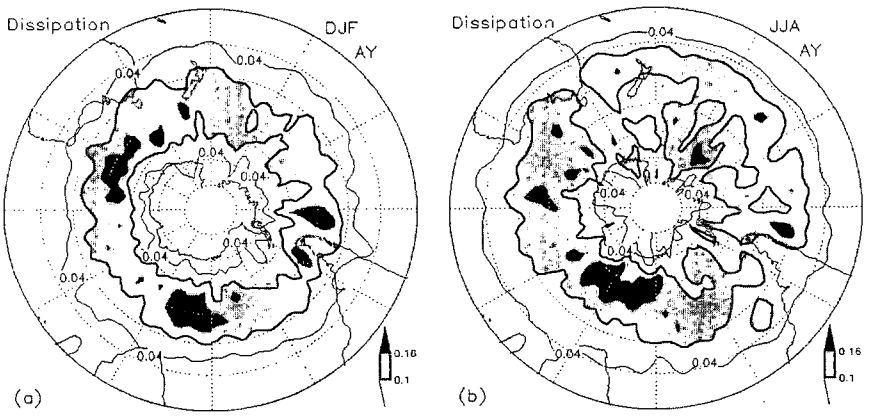

FIG. 11. Trough dissipation for season for (a) DJF and (b) JJA. Isolines are for 0.04, 0.1, and 0.16 troughs by season. Areas where the isolines are more than 0.1 troughs by season are darkened.

of the trough is less affected by stationary forcing than during the trough genesis.

The latitudinal distribution of the trough dissipation (figure not shown) shows that the 67.5°–40°S latitudinal belt is the main region of trough dissipation, with two maxima (one close to 57.5°S and the other at 52.5°S). The dissipation area diminishes toward the equator and the polar region. However, the reduction is greater in the polar direction. Comparing the latitudinal distribution of the trough dissipation with trough genesis, we noted that the dissipation curve is slightly inclined, accentuated to the equator, confirming that the dissipation process occurs more frequently in the lower latitudes compared with the genesis. Different from the genesis curve, the dissipation curve shows a steeper inclination to the polar region. The longitudinal distribution of trough dissipation (figure not shown) shows an almost homogeneity, except the relative maximum close to 160°E and the two minima at 50°E and 70°W (Fig. 10), which can be associated with the stationary long waves.

The seasonal variation of trough dissipation (Fig. 11) shows that over Antarctica the dissipation region is higher in MAM (figure not shown) and JJA, with a maximum of 0.16 troughs by season (Fig. 11b). Over the South Pacific Ocean to north of 40°S, the highest frequency of trough dissipation occurs in JJA. Over the South Atlantic close to South America there is a minimum of dissipation in MAM and in SON (figure not shown). LN95 observed that the trough dissipation was more frequent on the west side of mountain chains, and downstream of storm tracks. Over the southeastern Pacific close to South America one can note a maximum of trough dissipation during all the seasons, suggesting the influence of the Andes. On the other hand, it is not possible to locate the dissipation region of troughs in a specific region of storm tracks, that is, the trough dissipation can occur in any region in the 30°–70°S belt.

Comparing the dissipated trough distribution results of both winter and summer seasons with the KEA02 results we can observe some similarities and differences. KEA02 results show that the region to south of 60°S, including Antarctica, is the highest trough dissipation region, while in our results this region does not present a maximum of dissipation. Regions with agreement are observed over the central and southwestern Pacific Ocean to the north of 40°S and some regions over Antarctica. Another agreement is upstream of the Andes, where in our study we found the main maximum, while in KEA02 there was a secondary maximum. The Hoskins and Hodges (2005) wintertime results also show some agreements and some differences when compared with our study. As herein, their study presents an upper-level cyclonic track density band from the southeast of Australia to west of South America, but more to south. To the west of the Andes and to the south of Africa they also found maxima areas, but the last was dislocated more to south. Some areas identified by Hoskins and Hodges (2005) as dissipation were absent in our study, such as the subtropical band between Africa and Australia, the secondary maxima over the South Atlantic, and westward of the Antarctic Peninsula. Like KEA02's study, Hoskins and Hodges (2005) have shown the dissipation region displaced to higher latitude. Also, some of the differences between our results and those of others can be associated to sampling problems. In this study we used 24 yr (1979–2002) of data, while KEA02 used 40 yr (1958–97) of data. As observed by Simmonds and Jones (1998), in the SH middle and high latitudes there is considerable long-term variability of the semiannual oscillation.

The net trough distribution (genesis minus dissipa-

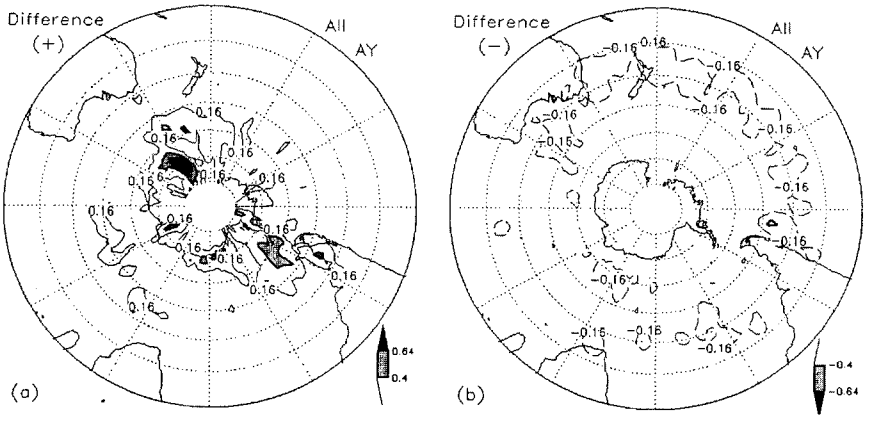

FIG. 12. Difference between genesis and dissipation of troughs for year: (a) positive and (b) negative difference. Isolines are for 0.16, 0.4, and 0.64 troughs per year. Areas where the isolines are more than 0.4 troughs per year are darkened.

tion) shows that the positive areas are more concentrated than the negative areas, which are spread in large areas in middle and subtropical latitudes (Fig. 12). The main positive regions are found over Antarctica, with a maximum of 0.64 troughs per year at 160°E and over the Drake Strait. The former region agrees with the stationary cyclone position observed by Inatsu and Hoskins (2004). Two secondary regions are found over South America and the southwest Indian Ocean close to 50°S (Fig. 12a). In the 50°–60°S latitude band, we observe three other positive areas upstream of the three stationary ridge waves (indicated by straight lines in Fig. 1a), which were observed by Van Loon and Jenne (1972) and Yasunari (1977). Similar features for negative areas cannot found, once they are more spread geographically (Fig. 12b). Negative areas are located over the South Atlantic Ocean, southern Australia, and the South Pacific Ocean, extending from Australia to South America around 40°S. Over the Pacific as well as the Atlantic Ocean, the negative areas show a spiral pattern on higher latitudes (Fig. 12b) close to the maximum 300-hPa synoptic time-scale kinetic energy region observed by Inatsu and Hoskins (2004).

The net seasonal variation of trough genesis shows a similar pattern for all seasons except summer, which has a different pattern (figure not shown). During DJF, both genesis and dissipation occur at any longitude in the 70°–30°S belt, in contrast to the other seasons that show preferential regions. Antarctica appears as a source of trough genesis during the period from autumn until spring, though mainly so in wintertime. Antarctica is more active at the 60°E, 160°E, and 60°W longitudes. KEA02's results also show Antarctica as a source region of troughs, mainly at 160°E and 60°W during wintertime, agreeing with the results of our study. The region enclosing the Drake Strait and the South Atlantic is revealed to be positive during all seasons, mainly in winter and spring. This last region is situated upstream of storm tracks, in agreement with LN95's result.

Sinclair (1997), Simmonds and Keay (2000a,b), and Wernli and Schwierz (2006) have shown that the surface cyclones that form between 30° and 50°S move to the polar region and suffer cyclolysis. In the trough case, our results show that the troughs that form in high latitudes dissipate in middle and subtropical latitudes, that is, the inverse meridional direction of the surface cyclones. Such a characteristic was also found by Grotjahn (1996).

a. Other relevant characteristics

The phase velocity of the trough varied from −7.0 to 28.0 m s^{-1}, with a mean of 13.6 m s^{-1} (Fig. 13). The phase velocity is higher in the middle and subtropical latitudes than in high latitudes, and the seasons with the

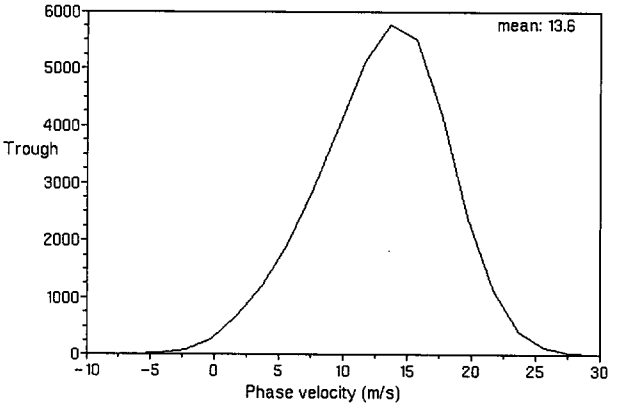

FIG. 13. Trough phase velocity (m s^{-1}).

TABLE 2. Trough phase velocity for latitude band and for season.

Season	Phase velocity ($m\ s^{-1}$) HL	ML	SL
DJF	7.8	15.0	11.6
MAM	7.4	15.2	12.3
JJA	8.3	15.0	14.0
SON	9.5	15.6	13.6

higher phase velocity are winter (SL) and spring (HL and ML) (Table 2). The mean phase velocity obtained by KEA02 was 14.0 $m\ s^{-1}$, with seasonal and latitudinal variation agreeing with our results, that is, with higher values of velocity in midlatitudes during the wintertime.

The zonal distance covered by the troughs was 5246 km on average (figure not shown), which represents 21% of the globe or 70° of longitude. There are a considerable number of troughs propagating more than 10^4 km; however, a few troughs had a long enough lifetime to complete a circle around the globe.

b. *Influence of El Niño/La Niña phenomena*

Several studies had shown that the SH flow is strongly influenced by El Niño–Southern Oscillation (ENSO) phase (Karoly 1989; Solman and Menéndez 2002; Rao et al. 2002) and interannual variability (Garreaud and Battisti 1999; Vera 2003). For example, the results of Solman and Menéndez (2002) show that over the eastern Indian Ocean and western Pacific Ocean the disturbances have higher amplitudes for EN than for LN events. Also, they show that the waves over the western Atlantic Ocean are partially fed by disturbances traveling along the subpolar branch of the Pacific Ocean storm tracks for EN events, while during the LN events the waves are fed only by disturbances from a subtropical branch. To evaluate the EN and LN influence on the trough behavior we presented differences of composite fields between EN events and NY, and between LN events and NY for all months, and for summer (DJF) and spring (SON) seasons (Figs. 14, 15, and 16, respectively).

During EN events, the positive values of trough occurrences are displaced to the north near 40°S (Fig. 14a) mainly over the South Pacific and South Atlantic Oceans. The occurrence of troughs over the southeast Pacific Ocean around 35°S was higher in EN events than in NY and LN events, but the opposite can be observed around 50°S (Fig. 14). Over southern Australia, southeastern Africa, and west of the Indian Ocean, the troughs are less frequent in EN events than in NY (Fig. 14a). During LN events (Fig. 14b) the troughs are more confined in a narrow latitudinal band (around 50°S) than in EN events and NY, forming a continuous band with values equal to or higher than eight troughs per year (figure not shown). This confinement can be a response to the stronger subpolar jet stream intensity and a weaker subtropical jet stream intensity that occurs in LN events (Karoly 1989). Therefore, in EN events, the subtropical jet stream tends to displace the wave troughs toward the equator from the subpolar jet stream, generating a scattered region of wave activity between the two jet streams (Nakamura and Shimpo 2004). Over southeastern South America, the northern part of Antarctica, and adjacent oceans the troughs are less frequently in LN events (Fig. 14b). In both composites, over southeastern Africa, southern Australia, and the adjacent ocean, we can observe a lesser trough appearance in LN and EN events than in NY (Fig. 14).

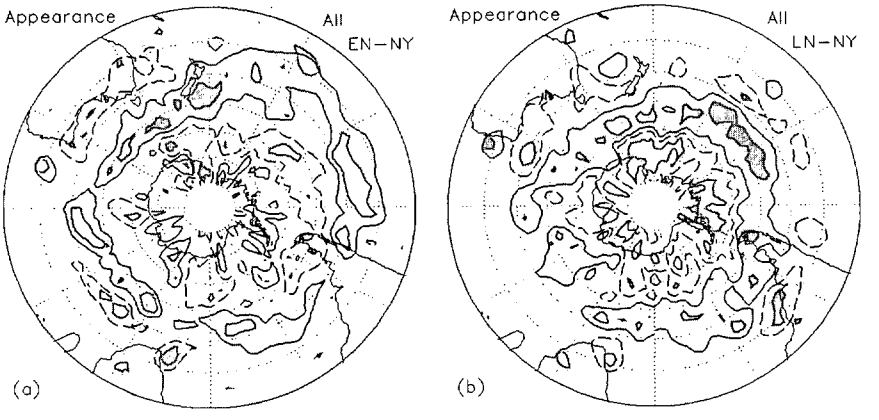

FIG. 14. Difference trough appearances between (a) EN and NY and (b) LN and NY. Solid lines indicate values equal to 0.5 troughs per year and broken lines indicate values equal to −0.5 troughs per year. Gray shade indicates areas with 95% significance level.

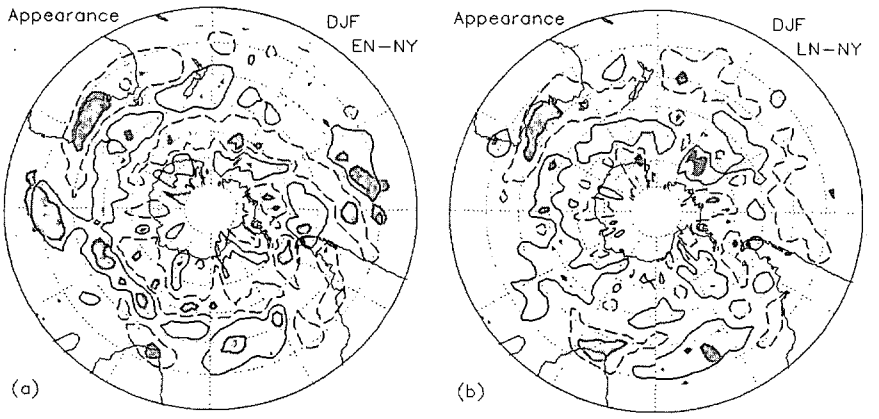

FIG. 15. As Fig. 14, but for DJF. Solid lines indicate values equal to 0.2 troughs per year and broken lines indicate values equal to −0.2 troughs per year.

Considering only DJF (Fig. 15), there is less trough occurrence in EN and LN events than in NY over southern Australia and adjacent oceans, and over southern Africa. To south of this region, we see a band starting from New Zealand and spreading to the west where more troughs are present in EN events than in NY (Fig. 15a). In most of this band there are more troughs in LN than NY (Fig. 15b). Over the central region of South Atlantic around 30° and 50°S more troughs occur in EN and LN events than in NY, while over the eastern South Pacific around 30° and 50°S there are more troughs in EN events than in NY and LN events.

During the SON period of EN events (Fig. 16) the troughs occur more frequently in the latitudinal band from 40° to 50°S over the western South Atlantic and eastern South Pacific and from 40° to 50°S over the Indian Ocean (Fig. 16a). Additionally, over the western South Pacific we can see that troughs are more frequently in EN and LN events than in NY. Over the Atlantic Ocean around 30°S there is a lesser trough appearance during LN events (Fig. 16b).

4. Conclusions

An objective method to identify and track 500-hPa mobile troughs was developed and applied to NCEP–NCAR reanalysis data for the period of 1 March 1979 through 28 February 2003. This method uses the Eulerian centripetal acceleration (ECA), as proposed by LN95. On average, 868 troughs per year were identified by the method, with an increasing trend during the period studied, especially after 1986. A positive tendency was also verified when we separate the trough series by season.

The seasonal variability shows that winter (summer) has higher (less) frequency of troughs. The troughs are normally found in the 60°–40°S latitudinal band, with

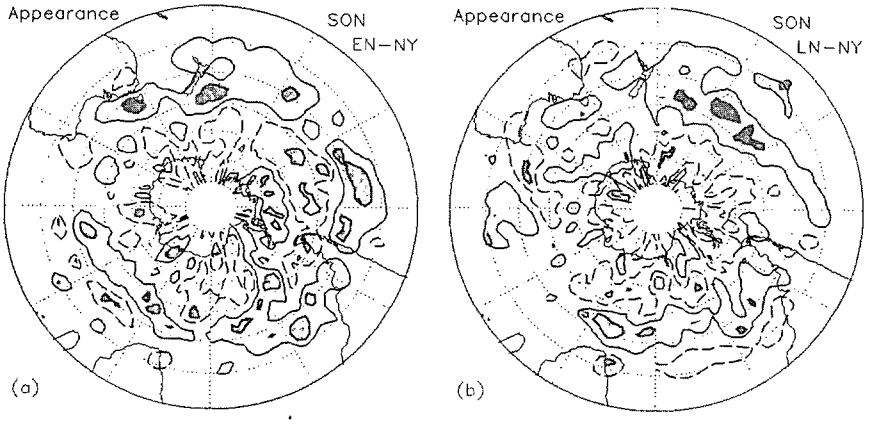

FIG. 16. As Fig. 14, but for SON. Solid lines indicate values equal to 0.2 troughs per year and broken lines indicate values equal to −0.2 troughs per year.

maximum at 50°S. During the summer, the trough activity is observed in a narrower latitude band, while in the winter this band extends from Antarctic to 30°S.

The longitudinal distribution shows that the trough genesis has three regions of maximum: one over the Drake Strait and the South Atlantic Ocean, the second over the Indian Ocean around 50°S, and the last one over the southwestern Pacific Ocean between 150°E and 150°W. These three maxima have a strong relationship with stationary wavenumber 3 identified by Van Loon and Jenne (1972). The seasonal variation of the trough genesis regions shows that Antarctica (eastern Pacific) becomes more (less) active during the winter.

The trough dissipation regions are shown to be less concentrated than the genesis regions, and present three maxima: one over the west of Andes, the second to the south of the African continent, and last to the south of Australia. The seasonal variation of the trough dissipations shows that the 30°–40°S band is more active during winter than in summer. The difference between genesis and dissipation phase is that the formation occurs more in the middle and high latitudes, while the dissipation is in the 40°–30°S latitude belt.

Based on these results, it is possible to conclude that the genesis is more concentrated in determined areas because these regions have connection with stationary waves and with local processes, such as baroclinic instability. However, in the dissipation phase it is not regulated by local processes, and is probably affected by other processes such as barotropic dissipation, downstream development, and the cascade of energy.

The troughs over the southeastern Pacific tend to be more confined around 50°S during La Niña events than in El Niño events. This confinement was associated with a less intense subtropical jet stream in La Niña events, because in El Niño events the subtropical jet stream tends to disperse the trough activity toward the equator from the subpolar jet stream.

Acknowledgments. This paper forms part of the Ph.D. thesis of the first author. Thanks are given to Coordenação de Aperfeiçoamento de Pessoal de Nível Superior (CAPES) for the Ph.D. scholarship to the first author. The authors thank Dr. J. W. Nielsen-Gammon for his help through electronic messages and the reviewers for their comments and suggestions.

REFERENCES

Carmo, A. M. C., 2004: Os strom tracks no Hemisfério Sul (Southern Hemisphere storm tracks). Ph.D. dissertation, Instituto Nacional de Pesquisas Espaciais, INPE-11585-TDI/962, 200 pp.

Chang, E. K. M., 2000: Wave packets and life cycles of troughs in the upper troposphere: Examples from the Southern Hemisphere summer season of 1984/85. *Mon. Wea. Rev.*, **128,** 25–50.

Fuenzalida, H. A., R. Sánchez, and R. Garreaud, 2005: A climatology of cutoff lows in the Southern Hemisphere. *J. Geophys. Res.*, **110,** D18101, doi:10.1029/2005JD005934.

Gan, M. A., and V. B. Rao, 1996: Case studies of cyclogenesis over South America. *Meteor. Appl.*, **3,** 359–369.

Garreaud, R. D., and D. S. Battisti, 1999: Interannual (ENSO) and interdecadal (ENSO-like) variability in the Southern Hemisphere tropospheric circulation. *J. Climate,* **12,** 2113–2123.

Gilbert, R. O., 1983: *Statistical Methods for Environmental Pollution Monitoring.* Van Nostrand Reinhold, 320 pp.

Grotjahn, R., 1996: Composite trough evolution of selected west Pacific extratropical cyclones. *Mon. Wea. Rev.*, **124,** 1470–1479.

Gutowski, W. J., Jr., L. E. Branscome, and D. A. Stewart, 1992: Life cycles of moist baroclinic eddies. *J. Atmos. Sci.*, **49,** 306–319.

Hodges, K. I., B. J. Hoskins, J. Boyle, and C. Thorncroft, 2003: A comparison of recent reanalysis datasets using objective feature tracking: Storm tracks and tropical easterly waves. *Mon. Wea. Rev.*, **131,** 2012–2037; Corrigendum, **132,** 1325–1327.

Hoskins, B. J., and K. I. Hodges, 2005: A new perspective on Southern Hemisphere storm tracks. *J. Climate,* **18,** 4108–4129.

Inatsu, M., and B. J. Hoskins, 2004: The zonal asymmetry of the Southern Hemisphere winter storm track. *J. Climate,* **17,** 4882–4892.

——, and ——, 2006: The seasonal and winter interannual variability of the split jet and storm-track activity minimum near New Zealand. *J. Meteor. Soc. Japan,* **84,** 433–445.

Innocentini, V., and E. D. Caetano Neto, 1996: A case study of the 9 August 1988 South Atlantic storm: Numerical simulations of the wave activity. *Wea. Forecasting,* **11,** 78–88.

James, I. N., 1988: On the forcing of planetary-scale Rossby waves by Antarctica. *Quart. J. Roy. Meteor. Soc.*, **114,** 619–637.

——, 1989: The Antarctica drainage flow: Implications for hemispheric flow on the Southern Hemisphere. *Antarct. Sci.*, **1,** 279–290.

Juckes, M. N., I. N. James, and M. Blackburn, 1994: The influence of Antarctica on the momentum budget of the southern extratropics. *Quart. J. Roy. Meteor. Soc.*, **120,** 1017–1044.

Kalnay, E., and Coauthors, 1996: The NCEP/NCAR 40-Year Reanalysis Project. *Bull. Amer. Meteor. Soc.*, **77,** 437–471.

Kanamitsu, M., W. Ebisuzaki, J. Woolen, J. Potter, and M. Fiorino, 1999: An overview of reanalysis-2. *Proc. Second Int. Conf. on Reanalyses,* Reading, United Kingdom, WMO, WCRP-109, WMO/TD-985, 1–4.

Karoly, D. J., 1989: Southern Hemisphere circulation features associated with El Niño–Southern Oscillation events. *J. Climate,* **2,** 1239–1252.

Keable, M., I. Simmonds, and K. Keay, 2002: Distribution and temporal variability of 500 hPa cyclone characteristics in the Southern Hemisphere. *Int. J. Climatol.*, **22,** 131–150.

Key, J. R., and A. C. K. Chan, 1999: Multidecadal global and regional trends in 1000 mb and 500 mb cyclone frequencies. *Geophys. Res. Lett.*, **26,** 2053–2056.

Lefevre, R. J., and J. W. Nielsen-Gammon, 1995: An objective climatology of mobile troughs in the Northern Hemisphere. *Tellus,* **47A,** 638–655.

Lim, E.-P., and I. Simmonds, 2007: Southern Hemisphere winter

extratropical cyclone characteristics and vertical organization observed with the ERA-40 data in 1979–2001. *J. Climate,* **20,** 2675–2690.

Marques, R. F. C., 1996: Bloqueio atmosférico no Hemisfério Sul (Southern Hemisphere atmospheric blocks). Ph.D. dissertation, Instituto Nacional de Pesquisas Espaciais, INPE-6742-TDI/632, 158 pp.

McBride, J. L., and Coauthors, 2005: Southern Hemisphere THORPEX science plan. WMO, 56 pp. [Available online at http://www.bom.gov.au/bmrc/mdev/staf/kkp/THORPEX/Shem_THORPEX_fin4.doc.]

Murray, R. J., and I. Simmonds, 1991: A numerical scheme for tracking cyclone centres from digital data. Part II: Application to January and July general circulation model simulations. *Aust. Meteor. Mag.,* **39,** 167–180.

Nakamura, H., and A. Shimpo, 2004: Seasonal variations in the Southern Hemisphere storm tracks and jet streams as revealed in a reanalysis dataset. *J. Climate,* **17,** 1828–1844.

Palmén, E., and C. W. Newton, 1969: Development of extratropical cyclones. *Atmospheric Circulation Systems: Their Structure and Physical Interpretation,* E. Palmén and C. W. Newton, Eds., Academic Press, 315–351.

Pezza, A. B., and T. Ambrizzi, 2003: Variability of Southern Hemisphere cyclone and anticyclone behavior: Further analysis. *J. Climate,* **16,** 1075–1083.

——, I. Simmonds, and J. A. Renwick, 2007: Southern Hemisphere cyclones and anticyclones: Recent trends and links with decadal variability in the Pacific Ocean. *Int. J. Climatol.,* **27,** 1403–1419.

Physick, W. L., 1981: Winter depression tracks and climatological jet streams in the Southern Hemisphere during the FGGE year. *Quart. J. Roy. Meteor. Soc.,* **107,** 883–898.

Piva, E. D., 2001: Estudo de caso sobre o papel dos fluxos de calor latente e sensível em superfície em processos de ciclogênese na costa leste ocorrida na costa da América do Sul (Case study about the latent and sensible surface heat fluxes during a cyclogenesis process occurred over the South American coast). M.S. thesis, Instituto Nacional de Pesquisas Espaciais, INPE-8498-TDI/781, 162 pp.

Rao, V. B., A. M. C. do Carmo, and S. H. Franchito, 2002: Seasonal variations in the Southern Hemisphere storm tracks and associated wave propagation. *J. Atmos. Sci.,* **59,** 1029–1040.

Salby, M. L., 1982: A ubiquitous wavenumber-5 anomaly in the Southern Hemisphere during FGGE. *Mon. Wea. Rev.,* **110,** 1712–1720.

Sanders, F., 1986: Explosive cyclogenesis over the west-central North Atlantic Ocean, 1981–1984. Part I: Composite structure and mean behavior. *Mon. Wea. Rev.,* **114,** 1781–1794.

——, 1988: Life history of mobile troughs in the upper westerlies. *Mon. Wea. Rev.,* **116,** 2629–2648.

Seluchi, M. E., 1995: Diagnóstico y pronóstico de situaciones sinópticas conducentes a ciclogénesis sobre el este de Sudamérica. *Geophis. Int.,* **34,** 171–186.

Simmonds, I., 2003: Modes of atmospheric variability over the Southern Ocean. *J. Geophys. Res.,* **108,** 8078, doi:10.1029/2000JC000542.

——, and D. A. Jones, 1998: The mean structure and temporal variability of the semiannual oscillation in the southern extratropics. *Int. J. Climatol.,* **18,** 473–504.

——, and R. J. Murray, 1999: Southern extratropical cyclone behavior in ECMWF analyses during the FROST special observing periods. *Wea. Forecasting,* **14,** 878–891.

——, and K. Keay, 2000a: Mean Southern Hemisphere extratropical cyclone behavior in the 40-year NCEP–NCAR reanalysis. *J. Climate,* **13,** 873–885.

——, and ——, 2000b: Variability of Southern Hemisphere extratropical cyclones behavior, 1958–97. *J. Climate,* **13,** 550–561.

Sinclair, M. R., 1995: A climatology of cyclogenesis for the Southern Hemisphere. *Mon. Wea. Rev.,* **123,** 1601–1619.

——, 1997: Objective identification of cyclones and their circulation intensity, and climatology. *Wea. Forecasting,* **12,** 595–612.

Solman, S. A., and C. G. Menéndez, 2002: ENSO-related variability of the Southern Hemisphere winter storm track over the eastern Pacific–Atlantic sector. *J. Atmos. Sci.,* **59,** 2128–2140.

Streten, N. A., and A. J. Troup, 1973: A synoptic climatology of satellite observed cloud vortices over the Southern Hemisphere. *Quart. J. Roy. Meteor. Soc.,* **99,** 56–72.

Trenberth, K. E., 1991: Storm tracks in the Southern Hemisphere. *J. Atmos. Sci.,* **48,** 2159–2178.

Uccellini, L. W., 1990: Processes contributing to rapid development of extratropical cyclones. *Extratropical Cyclones, The Erik Palmén Memorial Volume,* C. W. Newton and E. O. Holopainen, Eds., Amer. Meteor. Soc., 81–105.

Van Loon, H., 1965: A climatological study of the atmospheric circulation in the Southern Hemisphere during the IGY. Part I: 1 July 1957–31 March 1958. *J. Appl. Meteor.,* **4,** 479–491.

——, and R. L. Jenne, 1972: The zonal harmonics standing waves in the Southern Hemisphere. *J. Geophys. Res.,* **77,** 992–1003.

Vera, C., 2003: Interannual and interdecadal variability of atmospheric synoptic-scale activity in the Southern Hemisphere. *J. Geophys. Res.,* **108,** 8077, doi:10.1029/2000JC000406.

——, P. K. Vigliarolo, and E. H. Berbery, 2002: Cold season synoptic-scale waves over subtropical South America. *Mon. Wea. Rev.,* **130,** 684–699.

Wang, X. L., V. R. Swail, and F. W. Zwiers, 2006: Climatology and changes of extratropical cyclone activity: Comparison of ERA-40 with NCEP–NCAR reanalysis for 1958–2001. *J. Climate,* **19,** 3145–3166.

Watterson, I. G., and I. N. James, 1992: Baroclinic waves propagating from a high-latitude source. *Quart. J. Roy. Meteor. Soc.,* **118,** 23–50.

Wernli, H., and C. Schwierz, 2006: Surface cyclones in the ERA-40 dataset (1958–2001). Part I: Novel identification method and global climatology. *J. Atmos. Sci.,* **63,** 2486–2507.

Yasunari, T., 1977: Stationary waves in the Southern Hemisphere midlatitude zone revealed from average brightness charts. *J. Meteor. Soc. Japan,* **55,** 274–285.